Carbon 107 (2016) 268–272

Contents lists available at ScienceDirect

Carbon

journal homepage: www.elsevier.com/locate/carbon

Tunable magnetic moment and potential half-metal behavior of Fe-nanostructure-embedded graphene perforation

Huizhen Zhang [a, 1], Jia-Tao Sun [a, b, 1], Haifang Yang [a], Lin Li [a], Huixia Fu [a], Sheng Meng [a, b, *], Changzhi Gu [a, b, **]

[a] Beijing National Laboratory for Condensed Matter Physics, Institute of Physics, Chinese Academy of Science, Beijing 100190, China
[b] Collaborative Innovation Center of Quantum Matter, Beijing 100871, China

ARTICLE INFO

Article history:
Received 3 February 2016
Received in revised form
23 May 2016
Accepted 1 June 2016
Available online 2 June 2016

ABSTRACT

Doping with transition metal elements is an effective method to introduce magnetism in graphene, which could enable future graphene-based spintronic devices. Motivated by the recent experimental observation of a stable single layer iron membrane embedded in graphene perforation, we investigate the electronic and magnetic properties of the Fe-nanostructure-embedded graphene system based on first principles calculations. The results demonstrate that strain could lead to dramatic changes in the magnetic configurations for both small Fe clusters bonded to the edge carbon atoms of graphene perforation and the single layer Fe membrane fully embedded in the graphene layer. For optimal doping, a delicate balance can be achieved, which leads to a half-metallic electronic structure. This work suggests an easy and effective method to introduce and tune the magnetic properties of graphene, which offers a new direction for the development of future graphene-based spintronic devices.

1. Introduction

In the past decade graphene has attracted tremendous attentions thanks to its novel electronic and magnetic properties [1–5]. Besides its potential applications in nanoelectronics, new type of spintronic [6] devices has also been proposed, which may enable information storage, processing and communication at a faster speed, and with a lower energy consumption than conventional electronics [7]. Besides, the carbon-based spintronic devices may have an obvious advantage of long spin relaxation time because of the weak spin-orbit coupling (SOC) [8,9]. Doping transition-metal (TM) atoms in graphene is a straightforward way to make the spintronic application of graphene possible. Many theoretical [10–12] and experimental [13–15] studies have been focused on the transition-metal (TM)-atom-decorated graphene. Krasheninnikov et al. [11] reported that most of the TM metals embedded in graphene will introduce magnetic moments with strong bonding interaction. Based on high-resolution transmission electron microscopy, Gan et al. [15] and Cretu et al. [16] *etc.*, have observed that the TM metals bond strongly with graphene vacancy, suggesting it is an ideal stable candidate for future quantum devices applications. However, only separate and dispersed TM atoms were considered for all the above situations, which may present a limit on the magnetic moment, ferromagnetism, and the stability of the TM-dispersed graphene.

Zhao et al. [17] found that by electron-beam irradiation, Fe atoms can seal entirely small perforations in graphene and form a monolayer iron membrane. This is the first time to realize free-standing single-atom-thick Fe membrane, moving forward potential application of graphene in the fields of future spintronics and quantum information devices, due to the higher magnetic moment than its bulk counterpart, and a large perpendicular magnetic anisotropy [18], and so on. However, the magnetism for the embedded Fe-cluster/Fe-membrane in the graphene layer has yet to be comprehensively explored, which is central for the application of future spintronic devices.

Focusing on the Fe-nanostructure-embedded graphene layer, here we study the electronic and magnetic properties of these structures. Starting from two Fe atoms bonding to the edge carbon atoms of graphene perforation, we have investigated the Fe-graphene composite system by increasing the number of Fe

* Corresponding author. Beijing National Laboratory for Condensed Matter Physics, Institute of Physics, Chinese Academy of Science, Beijing 100190, China.
** Corresponding author. Beijing National Laboratory for Condensed Matter Physics, Institute of Physics, Chinese Academy of Science, Beijing 100190, China
E-mail addresses: smeng@iphy.ac.cn (S. Meng), czgu@iphy.ac.cn (C. Gu).
[1] The first two authors contributed equally to this work.

http://dx.doi.org/10.1016/j.carbon.2016.06.001
0008-6223/

atoms gradually, until the graphene perforation is filled completely by a freestanding Fe membrane. We found that large magnetic moments can be introduced by the Fe atoms and the neighboring C atoms. Our results show that the applied critical biaxial strain can change the total magnetism of the Fe-nanostructure-embedded graphene system dramatically. Interestingly, the magnetic moment will change abruptly more than once with increasing strain for the case of Fe membrane embedded in graphene. This provides a viable method to control the magnetic properties of graphene by strain for future spintronics, where the reliable control of the magnetic moment is a key step. Moreover, the combined system of iron cluster embedded in graphene perforation can be a half-metal, which afford an alternative method for achieving spin-polarized properties in graphene layer.

2. Methods

The density function theory calculations were performed to investigate the magnetic moments and electronic properties of the Fe-nanostructure-embedded graphene system using Vinnea Ab-initio Simulation Package (VASP) code. The projector augmented wave (PAW) pseudopotentials are adopted to describe the core-electrons interaction, and the Perdew-Burk-Ernzerhof (PBE) functional is adopted to describe the exchange and correlation potentials, which were proved to be correct to describe the TM-graphene systems well [11,19–21]. The cutoff energy 420 eV is used to expand the plane wave wavefunctions. The special points sampling integration over the Brillouin zone is employed by using the Monkhorst-Pack method with a $2 \times 2 \times 1$ K-point mesh. In the slab model, vacuum distance is about 20 Å between graphene plane. The force tolerance for geometry optimization is 0.01 eV/Å for the relaxed atoms. In addition, the Hubbard U corrected GGA calculations (GGA + U) [22] were performed to describe the partially localized Fe d orbitals, using the structure of Fe bonded with graphene hole edge as an example.

3. Results and discussions

When there are not enough Fe atoms to form the membrane, the Fe atoms will preferentially bond with the graphene edge, as observed in the experiment [14,23]. Fig. 1(a) shows the calculated ball-and-stick models of two Fe atoms bond with the hole edge of graphene. The system is magnetic with a total magnetic moment of 6 μ_B in this system. The distribution of magnetization density of this system as shown in Fig. 1(a) indicates that the magnetization mainly comes from the Fe atoms and partially from the adjacent carbon atoms. Since the collinear calculations have been carried out here, we anticipate that the adjacent C atoms' magnetic moments are parallel and antiparallel to Fe atoms' magnetic moments, depending on the electronic environment of each carbon. Fig. 1(b) shows the corresponding band structure of this system. The spin-up and spin-down state is non-degenerate, and both spin-up and spin-down states have no band gap.

Fig. 2(a) shows the ball-and-stick models and the spin density distribution for the configuration of four Fe atoms bonding with the periphery carbon atoms of graphene hole. It exhibits a magnetic state too with a total magnetic moment of 12 μ_B, twice than that of the previous. The spin density (Fig. 2(a)) in this case is mainly from embedded Fe atoms and adjacent C atoms, similar to the previous structure in Fig. 1(a). It is found that the distance dependence of the magnetic moment of carbon atoms around Fe nanocluster shows a trend like Friedel Oscillation. The corresponding band structure in Fig. 2(b) shows a gapped Dirac-cone like state denoted by the red and black dot. The partial charge densities in Fig. 2(c) and (d) indicate that the gapped Dirac-cone like state mainly comes from graphene and the d orbital of Fe atoms as shown in the distribution of partial charge densities. Fig. 2(e) shows the perspective view of the charge density in Fig. 2(d). Besides, only the spin up state is conductive around the Fermi level, and there is a gap for the spin down state as shown in Fig. 2(b). The system is half-metal for this configuration, suggesting an alternative method for achieving single spin device. When a smaller Hubbard U ($U \leq 2$) term is included, the system is still half-metallic. However it will not be half-metallic when a larger U term is considered. Nevertheless, the magnetic moments of the system are still 12 μ_B, not influenced by different U value persisting with our conclusions.

The strain effect for four iron atoms embedded graphene hole is studied. For the initial structure to be relaxed, we set a deviation of 0.1 Å out of the graphene plane for the Fe atoms, to take into account the possible undulation when compressed [24]. The strain-dependent magnetic moments are shown in Fig. 3(a). A biaxial strain β is defined here as $\beta = \frac{\Delta a}{a} \times 100\%$, where a is the lattice constant of graphene. The positive/negative β means the Fe-embedded graphene system is under tensile/compressive strain. When there is no strain applied on the system, the total magnetic moment of this system is 12 μ_B, about 0.113 μ_B per atom. When a biaxial compressive strain β is applied for the system, the magnetic ground state changes to lower spin state (0.075 μ_B per atom) abruptly at the strain of $\beta = -2\%$. The abrupt decrease in the magnetic moments of this system indicates that the iron-embedded graphene hole can be used as strain-mechanical membrane resonator [25].

Since the carbon atoms with magnetic moment are symmetric with respect to the vertical direction, all these periphery C atoms of graphene hole are classified into two types, C_1 and C_2, as shown in the inset of Fig. 3(d). The magnetic moment of each Fe and C_2 atoms decreases sharply at $\beta = -2\%$, as shown in Fig. 3(c) and (d). The magnetic moments of C_1 atoms increase at $\beta = -2\%$, but the variation is small in comparison to the Fe atoms and C_2 atoms. For the states of $\beta \geq -1\%$ or $\beta \leq -2\%$,the magnetic moment of Fe and C atoms change in the opposite trend, so the total magnetic moments remain the same for these states. We can see from Fig. 3(b) that the height of Fe atoms increase abruptly when $\beta = -2\%$, and the length of C–Fe bonds change suddenly at the same strain too. When the bond length changed abruptly, the magnetic moment changed spontaneously, which is consistent with previous reports on the single transition-metal atom embedded in graphene [26]. The abrupt change in the magnetic state is closely related to the structure change since the change of bond length between C–Fe and Fe–Fe affects the magnetic moment.

We now turn to the case of the complete Fe membrane embedded graphene hole. Fig. 4(a) shows the ball-and-stick models of the super cell. The initial structures are set up with a vertical displacement of 0.1 Å for the Fe atoms as in the situation of Fe atoms bonded to the graphene hole. The membrane contains six Fe atoms. Because of the confinement of the relatively smaller hole, the Fe atoms are not in the same plane and they distribute symmetrically up and down of the graphene plane after geometric relaxation, as can be seen in the cross-sectional view of Fig. 4(a). After comparing with the other configurations of Fe (all the Fe atoms in the same plane of graphene or all the Fe atoms deviation graphene plane on the same side), we found that this is the most stable structure.

Graphene is one of the strongest materials ever measured experimentally, and it has been demonstrated that it can sustain a strain as large as 25% [27,28]. Nevertheless similar stepped magnetic transition of the incomplete iron cluster embedded graphene hole is also found in this case but with significant difference as follows. There are more than one transition in magnetic moment for the embedded Fe-membrane. In the present work, the applied

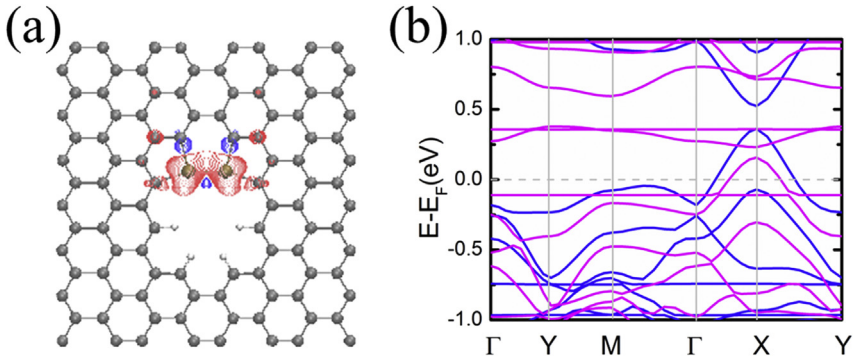

Fig. 1. (a) Geometries of the structure with two Fe atoms bond with the hole edge and the corresponding spin distribution. Gray, white, and brown balls denote carbon, hydrogen, and iron atoms respectively. Red/blue isosurface stands for spin accumulation/depletion. (b) Band structure for the configuration shown in (a). The blue (magenta) line denotes spin-up (spin-down) components. (A colour version of this figure can be viewed online.)

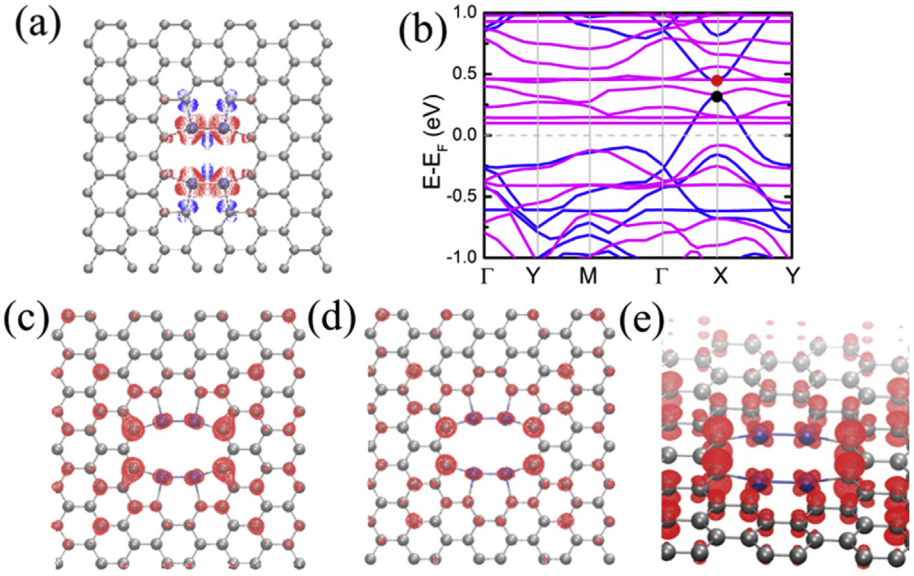

Fig. 2. (a) Ball-and-stick model of the structure with four Fe atoms bond with the hole edge and the corresponding spin distribution. Red/blue isosurface stands for spin accumulation/depletion. The gray and blue balls denote carbon and iron atoms respectively. (b) Band structure for the configuration shown in (a). The blue (magenta) line denotes spin-up (spin-down) components. (c) The charge density distribution for the state denoted by the black dot in panel (b). (d) The charge density distribution for the state denoted by the red dot in panel (b). (e) Perspective view of the charge density shown in Fig. 2(d). (A colour version of this figure can be viewed online.)

largest strain is 12%, as the Fe atoms will change the lattice structure of graphene when $\beta \geq 12\%$ (as shown in Fig. 4(d)). In Fig. 4 the ball-and-stick model at $\beta = 0\%$, 5%, 10% and 12% are presented as examples respectively. We can see from the side-view that the system tends to be more planar as the tensile strain increase as expected (thickness changes from 1.2 Å for strainless case to 0.07 Å for 12% strain).

When there is no strain applied on Fe-membrane embedded graphene system, the total magnetic moment of the system is 14 μ_B, about 0.13 μ_B per atom. When a tensile strain of $\beta = 3\%$ is applied for the system, the magnetic moment suddenly changes to 16 μ_B, or about 0.15 μ_B per atom. It can be further tuned to 20 μ_B abruptly when the strain is 10%, as shown in Fig. 5(a).

The six Fe atoms are classified into three types, designated as Fe-1, Fe-2, and Fe-3 in the inset of Fig. 5(c). The height and magnetic moment for Fe-1 and Fe-3 is degenerate except for the state of $\beta = 10\%$ (When $\beta = 10\%$, the Fe atoms move slightly downward in the graphene hole, and the system is not symmetric.). The magnetic moment of each Fe atom has the similar variation trend with the total magnetic moment. Accompanying the magnetic transition, the height and magnetic moments of each Fe atoms and bond length of Fe—Fe have similar trend, changing suddenly at $\beta = 3\%$ and 10%, too, as shown in Fig. 5(c) and (d).

It is interesting that the magnetic moment is closely related to the atomic structure from the above two cases. The magnetic moment mainly comes from the Fe *d* state and the adjacent dangling bonds of periphery carbon atoms. As the tensile/compressive strain changes the atomic structure, the bond length of the C—Fe and Fe—Fe will become longer/shorter, making the hybridization between them weaker/stronger. Then the electrons of Fe and C atoms will be unpaired/paired at a particular strain. Finally, the magnetic state is thus tuned. The principle of this sudden change in magnetism is similar to the situation of single TM atom embedded in graphene [26]. Nevertheless, this topic still requires more detailed studies.

It should be noted that there would be buckling instability for a compressive graphene sample even in the presence of embedded iron cluster [24]. Therefore, large compressive strain (>1%) in graphene samples might not be achievable based on current experimental techniques. This is not obvious within such a small supercell

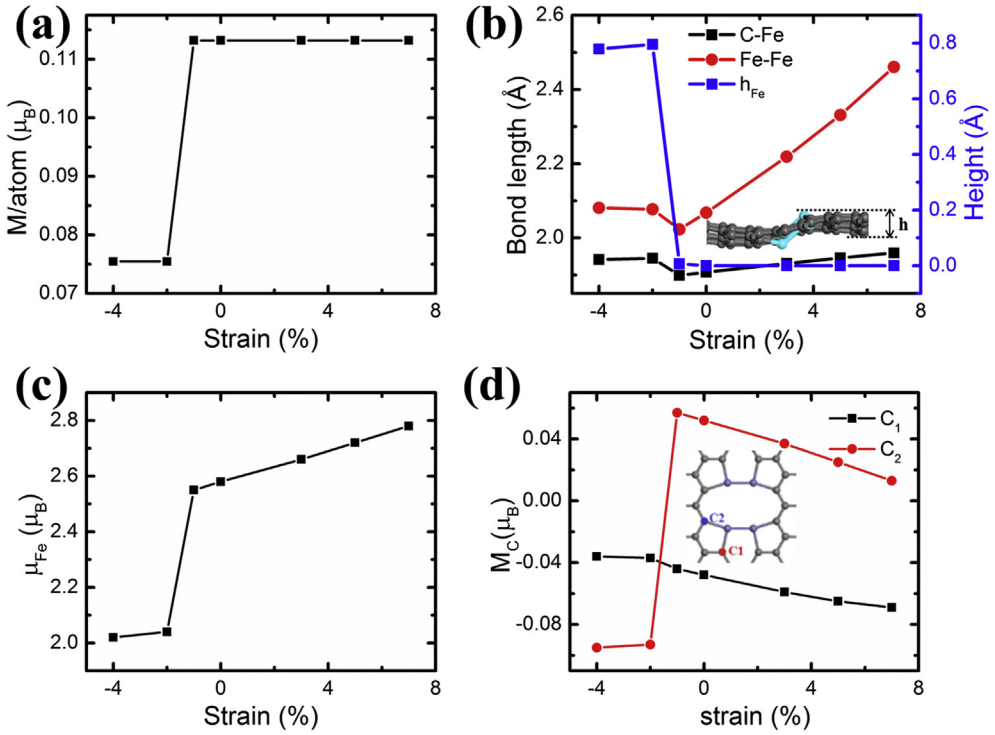

Fig. 3. Magnetic moment per atom (a), bond length (b), magnetic moment per Fe atom (c), magnetic moment of C_1 and C_2 (d), as a function of strain. The inset in (b) is the sketch of the height of Fe atoms. The inset in (d) denotes the C_1 and C_2 atoms. (A colour version of this figure can be viewed online.)

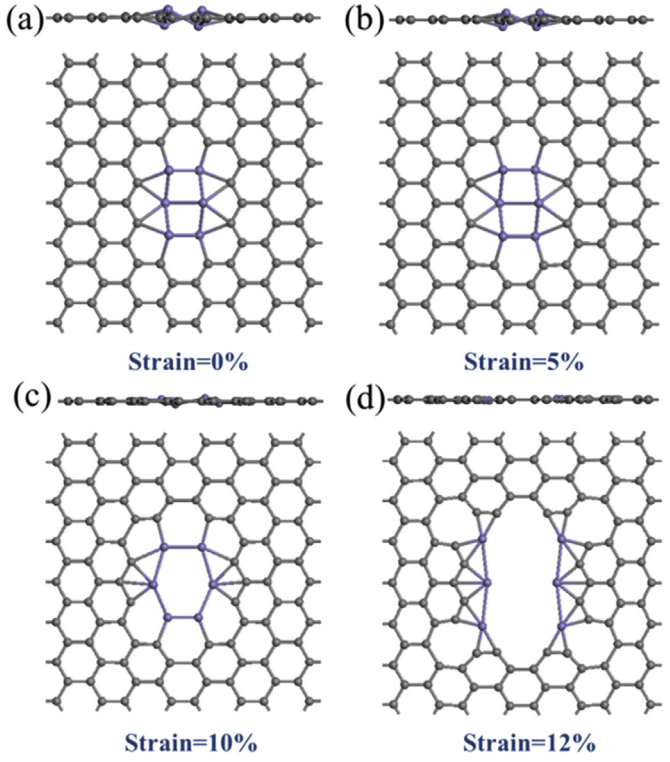

Fig. 4. Ball-and-stick models of the Fe-embedded graphene super cell for the applied strain = 0% (a), 5% (b), 10% (c) and 12% (d), respectively. Upper (lower) panel stands for a cross-sectional (top) view for each figure. Gray and blue balls denote carbon and iron atoms respectively. (A colour version of this figure can be viewed online.)

and the boundary condition considered in DFT calculations within this work, but ripples of large magnitude is easily observable in simulations when a compressive strain is applied in a large supercell size (~5 nm), to effectively eliminate the applied large in-plane compressive strain. Only for the sake of discussion and the completeness, we include here the data-set for compressive strain up to 4%. However, the buckling instability should be considered in the realistic applications, since the real graphene sample should have a size of ~100 nm or microns with free boundaries.

4. Conclusions

We have studied the electronic properties and magnetic moments of the Fe-graphene combined system based on first-principles calculations. Our results are generally consistent with the experimental observations on the single layer iron membrane within graphene perforations [17]. The system is magnetic, and the magnetic moment mainly comes from the Fe atoms and the adjacent C atoms. With the critical biaxial strain applied to the graphene membrane, the magnetic moment of the composite changed abruptly, for both the situations of Fe atoms bonded to the graphene edge only and the Fe nanomembrane entirely sealed in the graphene perforation. Besides, the magnetic moment can be changed more than one time with increasing strain for the case of Fe membrane embedded in graphene. The tunable magnetism can be attributed to the changes in the atomic structure, namely, the Fe–C and Fe–Fe bond lengths and the thickness of Fe-membrane. This provides a tunable magnetism in graphene for future spintronic applications. In particular, for the single layer Fe membrane first fabricated in experiment, simply applying a strain to control the magnetism is achievable. This work provides a useful clue for promoting graphene in future spintronic applications.

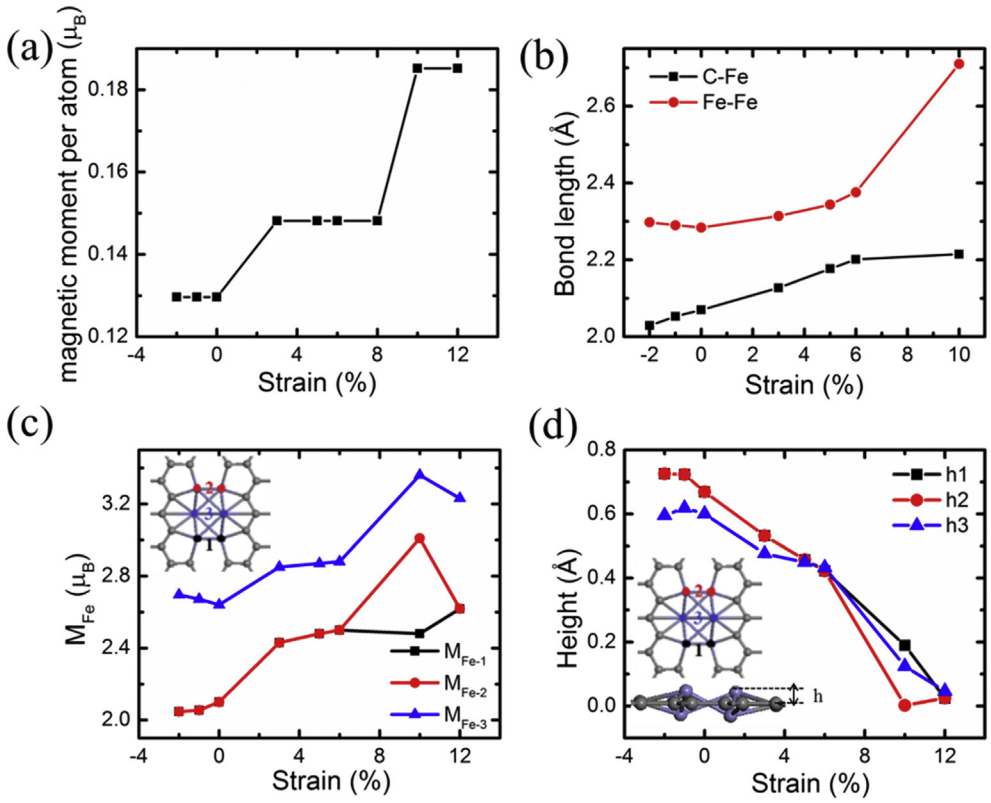

Fig. 5. Magnetic moment per atom (a), bond length (b), magnetic moment per Fe atom (c), height of each type of Fe atoms (d), as a function of strain. The inset in (c) and the upper inset in (d) denote the three types of Fe atoms. The bottom inset in (d) denotes the height of Fe atoms. (A colour version of this figure can be viewed online.)

Acknowledgements

The authors thank MOST (2012CB921403, 2013CBA01600), the National Natural Science Foundation of China (Grant Nos. 61390503, 51272278, 91323304, 61306114), and XDB07030100.

References

[1] A. H. Castro Neto, F. Guinea, N.M.R. Peres, K.S. Novoselov, A.K. Feim, The electronic properties of graphene, Rev. Mod. Phys. 81 (2009) 109–162.
[2] K.S. Novoselov, A.K. Geim, S.V. Morozov, D. Jiang, M.I. Katsnelson, I.V. Grigorieva, A.A. Firsov, Two-dimensional gas of massless dirac fermions in graphene, Nature 438 (2005) 197–200.
[3] K.S. Novoselov, A.K. Geim, S.V. Morozov, D. Jiang, Y. Zhang, S.V. Dubonos, I.V. Grigorieva, A.A. Firsov, Electric field effect in atomically thin carbon films, Science 306 (2004) 666–669.
[4] A.K. Geim, K.S. Novoselov, The rise of graphene, Nat. Mater 6 (2007) 183–191.
[5] D. Yu, E.M. Lupton, H.J. Gao, C. Zhang, F. Liu, A unified geometric rule for designing nanomagnetism in graphene 1 (2008) 497–501.
[6] Y.-W. Son, M.L. Cohen, S.G. Louie, Half-metallic graphene nanoribbons 444 (2006) 347–349.
[7] S. Power, M. Ferreira, Indirect exchange and ruderman–kittel–kasuya–yosida (RKKY) interactions in magnetically-doped graphene, Crystals 3 (2013) 49–78.
[8] D. Huertas-Hernando, F. Guinea, A. Brataas, Spin-orbit coupling in curved graphene, fullerenes, nanotubes, and nanotube caps, Phys. Rev. B 74 (2006) 155426.
[9] Y. Yao, F. Ye, X.L. Qi, S.C. Zhang, Z. Fang, Spin-orbit gap of graphene: first-principles calculations, Phys. Rev. B 75 (2007) 041401.
[10] B. Uchoa, V.N. Kotov, N.M.R. Peres, A.H. Castro Neto, Localized magnetic states in graphene, Phys. Rev. Lett. 101 (2008) 026805.
[11] A.V. Krasheninnikov, P.O. Lehtinen, A.S. Foster, P. Pyykkö, R.M. Nieminen, Embedding transition-metal atoms in graphene: structure, bonding, and magnetism, Phys. Rev. Let. 102 (2009) 126807.
[12] B. Uchoa, T.G. Rappoport, A. H. Castro Neto, kondo quantum criticality of magnetic adatoms in graphene, Phys. Rev. Lett. 106 (2011) 016801.
[13] V.W. Brar, R. Decker, H.M. Solowan, Y. Wang, L. Maserati, K.T. Chan, H. Lee, C.O. Girit, A. Zettl, S.G. Louie, M.L. Cohen, M.F. Crommie, Gate-controlled ionization and screening of cobalt adatoms on a graphene surface, Nat. Phys. 7 (2011) 43–47.
[14] J.A. Rodríguez-Manzo, O. Cretu, F. Banhart, Trapping of metal atoms in vacancies of carbon nanotubes and graphene, ACS Nano 4 (2010) 3422–3428.
[15] Y. Gan, L. Sun, F. Banhart, One- and two-dimensional diffusion of metal atoms in graphene, Small 4 (2008) 587–591.
[16] O. Cretu, A.V. Krasheninnikov, J.A. Rodríguez-Manzo, L. Sun, R.M. Nieminen, F. Banhart, Migration and localization of metal atoms on strained graphene, Phys. Rev. Lett. 105 (2010) 196102.
[17] J. Zhao, Q. Deng, A. Bachmatiuk, G. Sandeep, A. Popov, J. Eckert, M.H. Rümmeli, Free-standing single-atom-thick iron membranes suspended in graphene pores, Science 343 (2014) 1228–1232.
[18] J. Izquierdo, A. Vega, L.C. Balbas, D. Sanchez-Portal, J. Junquera, E. Artacho, et al., Systematic ab initio study of the electronic and magnetic properties of different pure and mixed iron systems, Phys. Rev. B 61 (2000) 13639–13646.
[19] E.J.G. Santos, A. Ayuela, D. Sánchez-Portal, First-principles study of substitutional metal impurities in graphene: structural, electronic and magnetic properties, New. J. Phys. 12 (2010) 053012.
[20] K.T. Chan, J.B. Neaton, M.L. Cohen, First-principles study of metal adatom adsorption on graphene, Phys. Rev. B 77 (2008) 235430.
[21] H. Sevincli, M. Topsakal, E. Durgun, S. Ciraci, Electronic and magnetic properties of 3d transition-metal atom adsorbed graphene and graphene nanoribbons, Phys. Rev. B 77 (2008) 195434.
[22] S.L. Dudarev, G.A. Botton, S.Y. Savrasov, C.J. Humphreys, A.P. Sutton, Electron-energy-loss spectra and the structural stability of nickel oxide: an LSDA+U study, Phys. Rev. B 57 (1998) 1505.
[23] C. Gong, A.W. Robertson, K. He, C. Ford, A.A. Watt, J.H. Warner, Interactions of Pb and Te atoms with graphene, Dalton. Trans. 43 (2014) 7442–7448.
[24] Y. Zhang, F. Liu, Maximum asymmetry in strain induced mechanical instability of graphene: compression versus tension, Appl. Phys. Lett. 99 (2011) 241908.
[25] D. Hatanaka, I. Mahboob, H. Okamoto, K. Onomitsu, H. Yamaguchi, An electromechanical membrane resonator, Appl. Phys. Lett. 101 (2012) 063102.
[26] B. Huang, J. Yu, S.H. Wei, Strain control of magnetism in graphene decorated by transition-metal atoms, Phys. Rev. B 84 (2011) 075415.
[27] C. Lee, X. Wei, J.W. Kysar, J. Hone, Measurement of the elastic properties and intrinsic strength of monolayer graphene, Science 321 (2008) 385–388.
[28] K.S. Kim, Y. Zhao, H. Jang, S.Y. Lee, J.M. Kim, K.S. Kim, J.H. Ahn, P. Kim, J.Y. Choi, B.H. Hong, Large-scale pattern growth of graphene films for stretchable transparent electrodes, Nature 457 (2009) 706–710.